Supplementary Materials

Ba-mediated Pt/TiO_2 for Enhanced Low Temperature HCHO Oxidation Originated from The Interaction between Pt and Ba

Chenxuanzhi Ruan [1,2], Hongguo Gao [1], Xuejuan Zhao [2], Zelin Hua [1], Shenjie Lv [1], Shanshan Chen [3,*], and Licheng Li [1,*]

[1] Jiangsu Co-Innovation Center of Efficient Processing and Utilization of Forest Resources, College of Chemical Engineering, Nanjing Forestry University, Nanjing 210037, China
[2] School of Materials Science and Engineering, Nanjing Institute of Technology, Nanjing 211167, China
[3] School of Materials Science and Engineering, Nankai University, Tianjin 300350, China
* Correspondence: sschen@nankai.edu.cn (S.C.); lilc@njfu.edu.cn (L.L.)

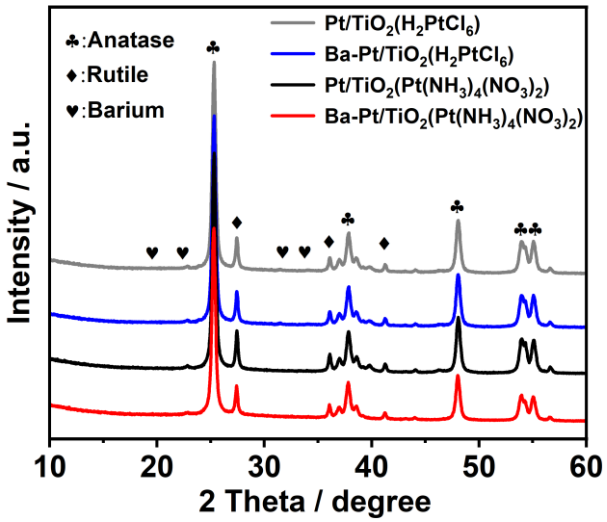

Figure S1. XRD patterns of Pt/TiO_2(H_2PtCl_6), Ba-Pt/TiO_2(H_2PtCl_6), Pt/TiO_2($Pt(NH_3)_4(NO_3)_2$) and Ba-Pt/TiO_2($Pt(NH_3)_4(NO_3)_2$).

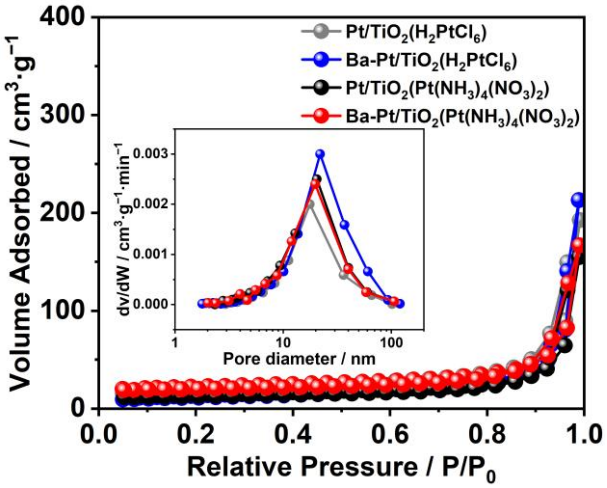

Figure S2. N_2 adsorption/desorption isotherms of Pt/TiO_2(H_2PtCl_6), Ba-Pt/TiO_2(H_2PtCl_6), Pt/TiO_2($Pt(NH_3)_4(NO_3)_2$) and Ba-Pt/TiO_2($Pt(NH_3)_4(NO_3)_2$). Inserted diagram shows the pore size distribution curves of four samples.

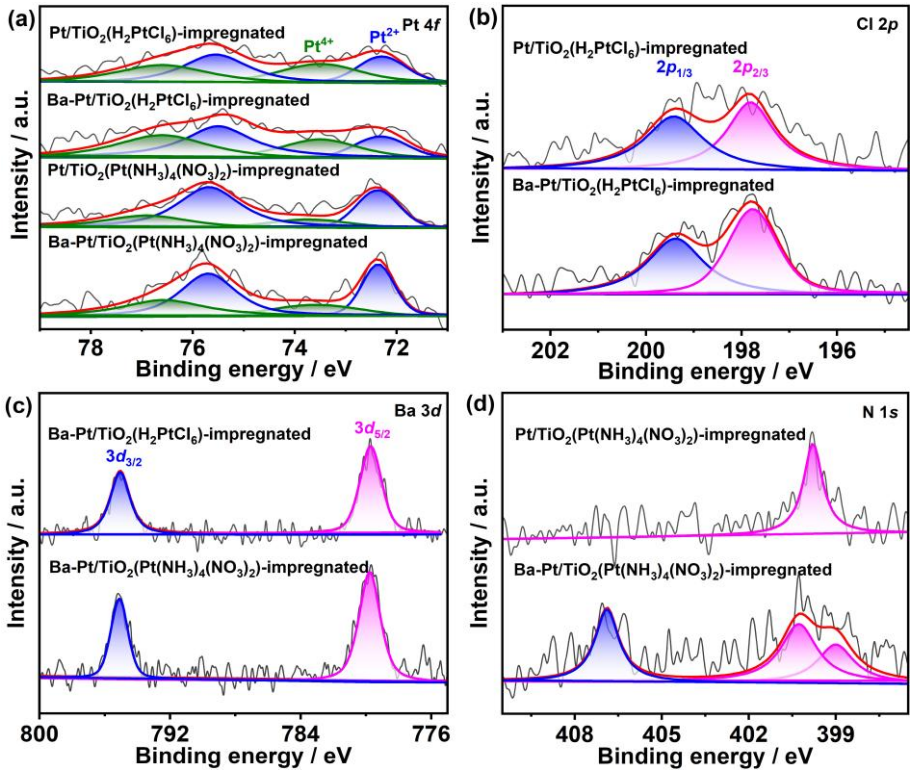

Figure S3. XPS spectra for Pt 4*f* (c), Cl 2*p* (d), Ba 3*d* (e), N 1*s* (f) of various impregnated samples.

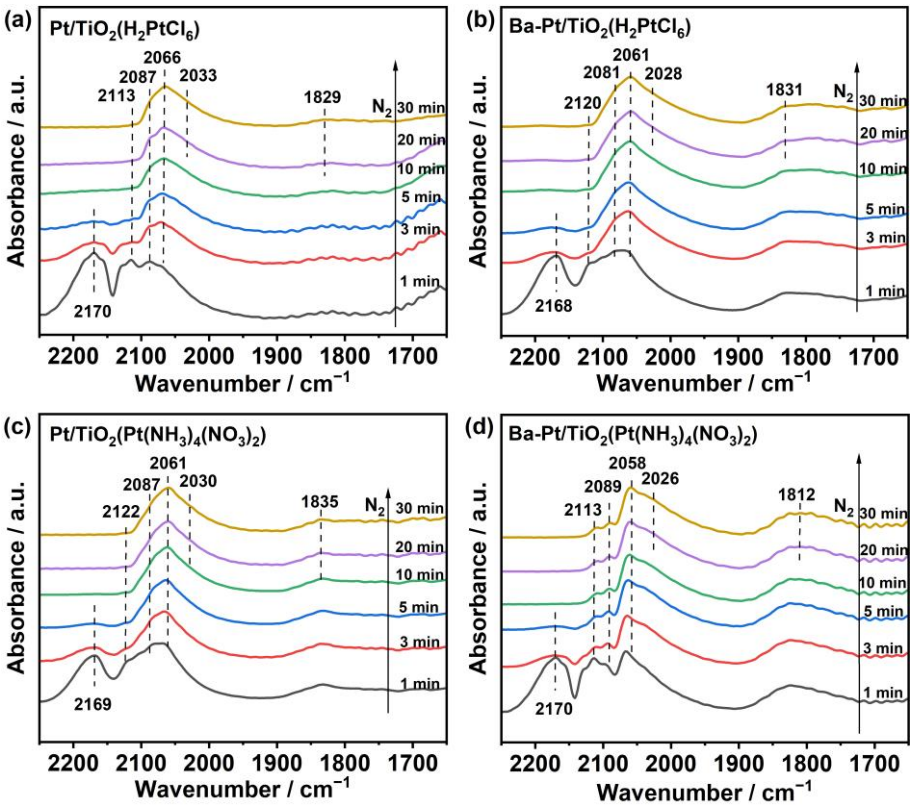

Figure S4. The dynamic CO adsorption *in situ* DRIFTS of $Pt/TiO_2(H_2PtCl_6)$ (a), $Ba\text{-}Pt/TiO_2(H_2PtCl_6)$ (b), $Pt/TiO_2(Pt(NH_3)_4(NO_3)_2)$ (c) and $Ba\text{-}Pt/TiO_2(Pt(NH_3)_4(NO_3)_2)$ (d) catalysts with N_2 purge.

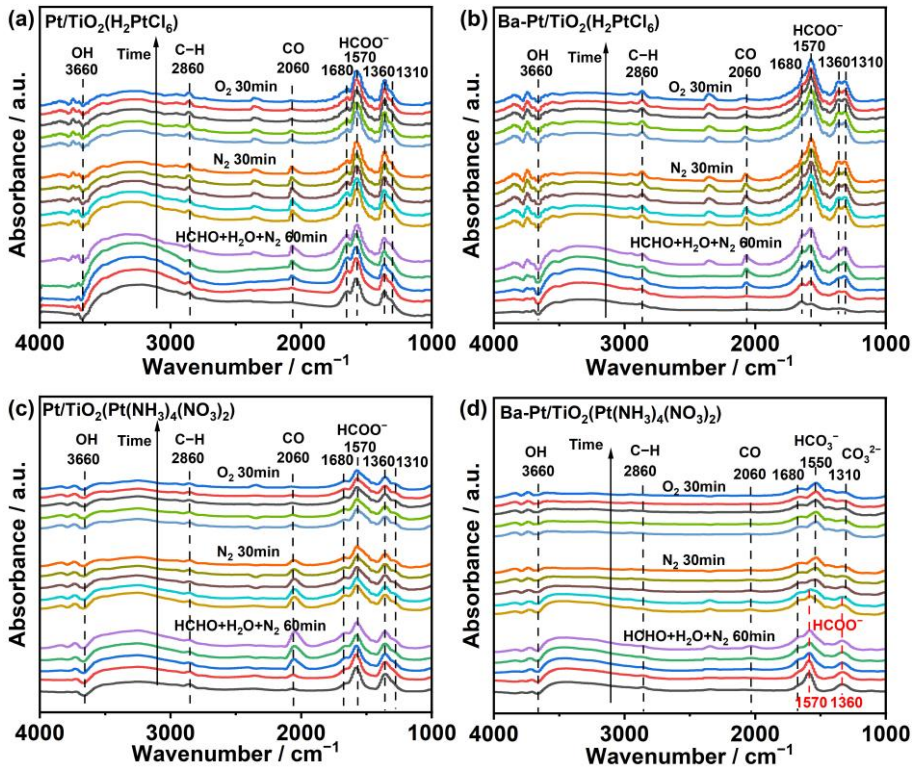

Figure S5. HCHO-DRIFTS spectra of Pt/TiO$_2$(H_2PtCl_6) (a), Ba-Pt/TiO$_2$(H_2PtCl_6) (b), Pt/TiO$_2$(Pt(NH$_3$)$_4$(NO$_3$)$_2$) (c) and Ba-Pt/TiO$_2$(Pt(NH$_3$)$_4$(NO$_3$)$_2$) (d) with a flow of HCHO+H_2O+N_2 for 60 min, N_2 purging for 30 min, and finally O_2 purging for 30 min.

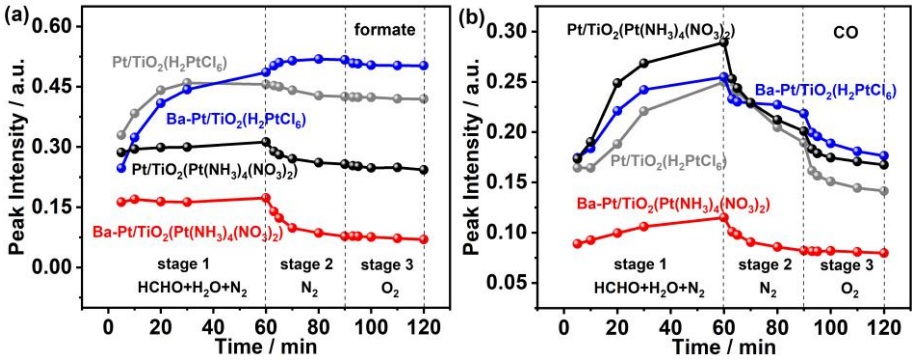

Figure S6. The band intensities of formate (a) and CO (b) as a function of time for Pt/TiO$_2$(H_2PtCl_6), Ba-Pt/TiO$_2$(H_2PtCl_6), Pt/TiO$_2$(Pt(NH$_3$)$_4$(NO$_3$)$_2$) and Ba-Pt/TiO$_2$(Pt(NH$_3$)$_4$(NO$_3$)$_2$).

Table S1. Physicochemical properties of various catalysts.

Sample	S_{BET} ($m^2 \cdot g^{-1}$)	V_P ($cm^3 \cdot g^{-1}$)	D_P (nm)	H_2-TPR information$^{\beta}$
				Lower peak
Pt/TiO$_2$(H_2PtCl_6)	46.87	0.29	13.9	1.00
Ba-Pt/TiO$_2$(H_2PtCl_6)	44.56	0.27	14.3	1.28
Pt/TiO$_2$(Pt(NH$_3$)$_4$(NO$_3$)$_2$)	41.78	0.24	15.1	0.97
Ba-Pt/TiO$_2$(Pt(NH$_3$)$_4$(NO$_3$)$_2$)	40.84	0.23	15.4	2.52

β: The H_2 desorption amount was evaluated by a normalization method. Low peak was less than 200 °C.

Table S2. Summarized XPS data of various catalysts.

Samples	BE of Pt^0 $4f_{7/2}$ (eV)	$Pt^0/(Pt^0+Pt^{2+}+Pt^{4+})$ (%)	$Pt^{2+}/(Pt^0+Pt^{2+}+Pt^{4+})$ (%)	BE of Ba $3d_{5/2}$ (eV)	BE of Ba $3d_{3/2}$ (eV)	O_{II}/O_I	OH/O_I
Pt/TiO$_2$(H_2PtCl_6)	71.1	41	28	-	-	0.33	0.25
Ba-Pt/TiO$_2$(H_2PtCl_6)	71.2	42	30	779.1	794.6	0.33	0.25
Pt/TiO$_2$(Pt(NH$_3$)$_4$(NO$_3$)$_2$)	71.1	41	29	-	-	0.33	0.22

Ba-$Pt/TiO_2(Pt(NH_3)_4(NO_3)_2)$	71.2	39	41	780.0	795.5	0.43	0.31
Ba/TiO_2	-	-	-	779.1	794.6	-	-

BE: binding energy.

The TOF value of various catalysts was calculated according to the following formula.

$$TOF = \frac{\text{Reaction rate}/10^6}{\frac{1}{M_{Pt}} \times D}$$

where M_{Pt} (195 g/mol) is the relative molecular mass of Pt.

The dispersion of Pt nanoparticles can be calculated according to the following equation.

$$D = 6\frac{v_m/a_m}{d}$$

where D is the dispersion of Pt nanoparticles, a_m (8.07 Å^2) denotes a surface atom, v_m (15.10 Å^3) represents the volume occupied by each atom in the bulk metal, d (nm) signifies the average particle size of Pt.